Demonstration of an iron fluorescence lidar operating at 372 nm wavelength using a novel Nd:YAG laser

BERND KAIFLER[1,*], CHRISTIAN BÜDENBENDER[1], PETER MAHNKE[2], MATTHIAS DAMM[2], DANIEL SAUDER[2], NATALIE KAIFLER[1], AND MARKUS RAPP[1]

[1] *Deutsches Zentrum für Luft- und Raumfahrt (DLR), Institut für Physik der Atmosphäre, Oberpfaffenhofen, Germany*
[2] *Deutsches Zentrum für Luft- und Raumfahrt (DLR), Institut für Technische Physik, Stuttgart, Germany*
[*] *Corresponding author: bernd.kaifler@dlr.de*

Compiled June 27, 2017

We report on the development of a pulsed Nd:YAG laser operating at 1116 nm wavelength. Because the third harmonic is within a few GHz of the 372 nm absorption line of iron, this laser system represents an alternative to alexandrite lasers commonly used in iron fluorescence lidars. With our prototype we achieved 0.5 W at 372 nm wavelength and 100 Hz pulse repetition frequency. As a proof of concept, we show iron density measurements which have been acquired using the novel lidar transmitter.

OCIS codes: *(101.3920) Meteorology; (010.3640) Lidar; (300.2530) Fluorescence, laser-induced; (140.2020) Diode lasers; (140.3530) Lasers, neodymium; (140.3540) Lasers, Q-switched; (140.3600) Lasers, tunable*

http://dx.doi.org/10.1364/ao.XX.XXXXXX

Metal fluorescence lidar systems have been used to observe atmospheric metal layers between approximately 80 and 120 km altitude for almost 50 years. Starting in 1968, flashlamp-pumped dye lasers were used to probe the sodium layer at 589 nm wavelength and detect its fluorescence [1]. The laser systems at that time were spectrally rather broad and therefore did not allow for resolution of the fine structure of sodium. First successful measurements of sodium temperature based on probing of the Doppler-broadened Na D_1 and D_2 lines were reported in 1979 [2]. Since then, sodium lidar systems have been steadily improved, providing better altitude and time resolutions as well as higher accuracy of atmospheric temperature and even wind measurements in an otherwise rather inaccessible region of the atmosphere [3–9]. The spectroscopy of sodium is discussed in detail in a recent review paper [10].

First observations of iron fluorescence at 372 nm were obtained with dye lasers in the late eighties and early nineties [11, 12]. Observations with an iron Boltzmann lidar which uses two wavelengths 372 nm and 374 nm to derive atmospheric temperature commenced in 1999 [13]. Doppler temperature measurements were reported in 2004, albeit at a different wavelength of 386 nm [14]. The absorption line at 386 nm is approximately half as strong as that at 372 nm, however the longer wavelength can be easily generated by a frequency-doubled alexandrite laser. The lidar system described in [14] represents a first successful attempt to replace the high maintenance dye lasers with a solid-state laser. Availability of reliable and low maintenance lasers is a critical prerequisite for metal lidar systems designed for long-term observations of mesospheric temperature at remote locations (see e.g. [15]), as well as for the new class of fully autonomous lidar systems currently under development. Unlike sodium, iron has no hyperfine structure and the absorption cross-section is approximately 73 times weaker, thus allowing the use of much higher laser power densities without saturation and accompanying deformation of the shape of the probed absorption line. This is especially important for lidars capable of observing in daylight, since a common method to reduce the solar background is making the field of view smaller, leading automatically to higher power densities. The development of powerful, reliable and compact lidar transmitters for 372 nm wavelength is therefore crucial for the next generation of middle atmosphere temperature and wind lidars.

As a coincidence of nature, one of the weaker Nd:YAG emission lines lies at 1115.95 nm wavelength which is within a few GHz of the tripled wavelength of the absorption line of iron at 372 nm [16]. This coincidence is virtually asking for exploitation, as compact and powerful diode-pumped Nd:YAG lasers are readily available nowadays. Indeed, several studies demonstrated successful operation of Nd:YAG lasers at 1116 nm wavelength [17, 18]. All of these studies utilized laser systems which were either operated in CW mode or with pulse repetition rates exceeding 10 kHz. For the application in metal lidar systems, however, the time the laser pulse needs to propagate in the atmosphere up to the mesosphere/lower thermosphere and back to the ground limits the usable pulse repetition frequency to about 500 Hz. We demonstrate a prototype laser system capable of producing 13 mJ at 1116 nm wavelength, 900 ns pulse length and 100 Hz pulse repetition frequency. Furthermore, as a proof of concept, we show lidar observations at 372 nm wavelength using this laser prototype.

The overall layout of the laser system is shown in Fig. 1. The laser was configured as linear stable cavity with one of the end mirrors mounted on a piezo stack for cavity length control. Both end mirrors were coated for high reflectivity at 1116 nm wavelength and low reflectivity at 1064 nm and 1319 nm. A

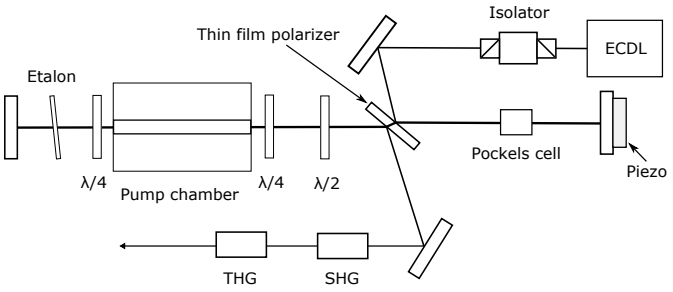

Fig. 1. Schematics of the laser system.

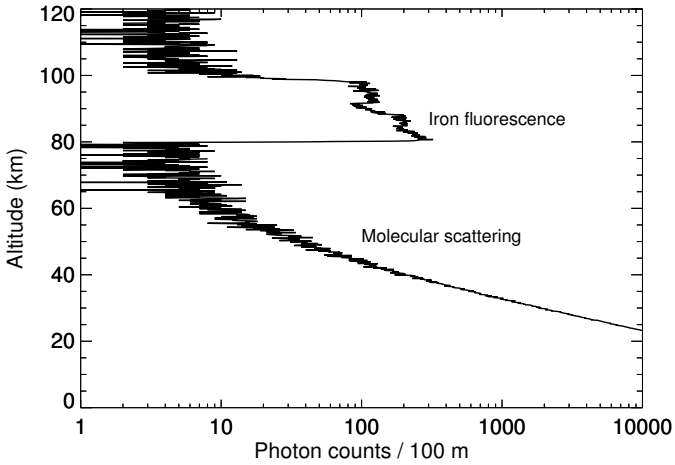

Fig. 2. Backscatter profile of the first lidar observation using the new Nd:YAG-based laser system. The data were acquired at DLR Oberpfaffenhofen on 11 November 2015 between 20:04 and 20:13 UT.

diode-side-pumped pump chamber from Rofin was located near the center of the 80 cm long cavity. To prevent spatial hole burning, a quarter-wave plate was inserted at each side of the pump chamber and an etalon was used to suppress modes at unwanted wavelengths. The polarizer served as output coupler and input coupler for the seed beam. The output coupling efficiency was controlled with the half-wave plate. Finally, a Pockels cell was located between the polarizer and the piezo mirror. Conversion to 372 nm wavelength was achieved through subsequent second harmonic (SHG) and third harmonic generation (THG).

The seed laser was an extra cavity diode laser (ECDL) from Newport with 50 mW power at 1116 nm wavelength. This ECDL has a continuous mode hop-free tuning range of 55 GHz and a frequency drift of less than 240 MHz/h. A Faraday isolator with 60 dB isolation was used to prevent the oscillator from backfiring into the seed laser. A high-speed InGaAs photodiode in combination with a 1 GHz digital oscilloscope was used to record and analyze time traces of the optical pulses.

Single longitudinal mode operation was achieved by mode-matching the laser cavity to the seed laser. Here, the voltage of the piezo was manually adjusted until the pulse buildup time was minimal (minimalization of pulse buildup time technique). We analyzed the time traces of the optical pulses by computing the fast Fourier transform and looked for signs of longitudinal mode beating. With the laser properly aligned and the pulse buildup time minimized, the power of the largest side mode was 30 dB smaller compared to the main mode. After about 1 hour of operation, the setup was stable enough that the laser remained seeded for several minutes without the need for further adjustments to the cavity length. The pulse energy was 5 mJ at 372 nm wavelength and 100 Hz pulse repetition frequency. A more detailed description and characterization of the laser system will be published in a separate study.

The first lidar observation using the prototype laser system was carried out at the DLR site in Oberpfaffenhofen, southern Germany, on the night of 11 November 2015. The laser beam was directed vertically into the sky next to the 406 mm diameter receiving telescope (Meade 16" LightBridge, 1829 mm focal length). A fiber with 550 µm core diameter mounted in the focal spot of the telescope guided the collected backscattered light to the receiver which comprises an aspheric collimation lens with 20 mm focal length, a 1 nm wide interference filter with approximately 80% transmission, and a photo multiplier tube for detection (Hamamatsu H10682-210). The electrical signal was recorded using a multi-channel analyzer with 2 ns time resolution (FAST ComTec P7888). To protect the photo multiplier from overloading, a mechanical chopper running at 300 Hz was inserted between the fiber end and the collimation lens. The phase delay between the chopper and the laser pulse was adjusted such that the chopper blocked the backscattered light from below 18 km altitude.

We tuned the laser to the ^{56}Fe vacuum wavelength 372.099 nm using a calibrated wavemeter (HighFinesse WSU10) and manually stabilized the laser cavity to the seeder as discussed in the previous section. Fig. 2 shows the backscatter profile with 100 m vertical resolution integrated between 20:04 and 20:13 UT. Fluorescence of atmospheric iron is visible as broad peak between 81 and 102 km altitude, whereas the strong signal below 70 km originates from molecular scattering at air molecules. The flat background above 110 km comes mostly from noise, e.g. residual sky brightness and detector dark counts, and very little resonance scattering.

We verified single longitudinal mode operation of the laser during the whole observation period by monitoring the pulse power spectrum and the pulse buildup time. Tuning the laser wavelength slowly away from the iron line resulted in a gradual decrease of detected fluorescence until no fluorescence could be detected any more (not shown). The scan revealed no obvious side bands in the laser spectrum. If present, such sidebands should have manifested themselves during the wavelength scan as sudden increase in fluorescence when the central wavelength is tuned away from the iron line. The central portion of one of these wavelength scans is shown in Fig. 3. Here, photon counts are integrated for approximately one minute per sampled frequency during which times the laser wavelength was held constant. The error bars mark the uncertainty $\sqrt{N}$ of the integrated signal, where N is the number of detected photons. By fitting a model to the acquired fluorescence spectrum, we could determine the Doppler width and corresponding iron temperature 262 K, albeit with a large statistical uncertainty of approximately 19 K. Taking the uncertainty into account, the derived iron temperature is still significantly larger than the temperature 229 K at 85 km altitude measured by the SABER instrument onboard the TIMED satellite 9.7 h later (orbit No. 75480, 12 Nov 2015 05:31 UT, 100 km north of the lidar). The deviation is not surprising given that it took us 14 minutes to manually scan across the iron absorption line, and measured iron densities are likely to change in this time frame due to chemical processes and advection, thereby altering the apparent line shape. This problem will

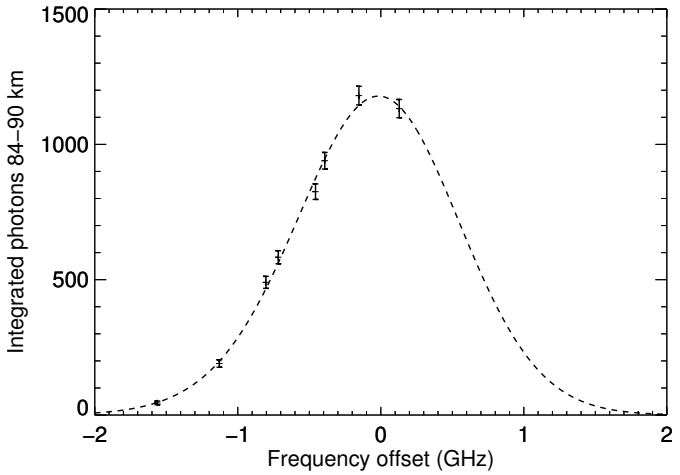

Fig. 3. Spectrum of the iron absorption line at 372 nm obtained by scanning the lidar wavelength and recording the return signal from the iron layer between 19:39 and 19:53 UT. The integration period for each sampled frequency was approximately one minute. The broken line shows the modeled spectrum for 262 K temperature.

be solved with the implementation of cavity control techniques (e.g. ramp and fire [19]) which allow for much faster scan rates in the order of few seconds. When retrieving the atmospheric temperature from the spectrum shown in Fig. 3 we assumed a spectral width of the laser of 30 MHz (FWHM). Increasing the line width to 79 MHz reduces the retrieved temperature to 229 K which is the value reported by the SABER instrument. Thus, a spectrally broader laser could potentially explain the observed temperature offset. However, since the assumption of a spectrally broad laser has no significant effect on the calculated statistical uncertainty of the derived temperature which is much larger compared to estimates based on photon count statistics, we conclude that the temperature offset observed in our observation is most likely caused by chemical processes and advection rather than underestimation of the spectral width.

In conclusion, we demonstrated a new laser concept using a Nd:YAG laser for generation of pulsed light at 372 nm wavelength. This wavelength is of special interest as it can be used to probe a strong Doppler broadened absorption line of iron to determine iron density as well as atmospheric temperature and line of sight winds at mesospheric altitudes [20]. Other groups have shown that iron Doppler measurements at 386 nm wavelength are possible using narrowband tunable alexandrite lasers [14]. The experimental demonstration of Doppler temperature and wind measurements at 372 nm wavelength is still outstanding, however. The use of the shorter wavelength is attractive because the absorption line at 372 nm is approximately twice as strong as at 386 nm. Thus, a lidar operating at 372 nm receives twice the signal for the same laser power, allowing for shorter integration periods and higher vertical resolutions. The test run of our experimental lidar system demonstrated the suitability of our laser design for atmospheric iron density measurements at 372 nm (see Fig. 2). With the laser in its current configuration, we are not able to tune the laser wavelength with the precision and speed required for Doppler measurements while maintaining single longitudinal mode operation of the laser. This shortcoming will be solved in near future with the implementation of laser cavity control techniques (e.g. ramp and fire). Further improvements target the beam expander and telescope. Tests showed that the telescope was not properly focused during the observation and the divergence of the laser beam (0.6 mrad) was approximately twice as large as the field of view of the telescope. This lead to a significant loss of signal which can be easily reduced using an improved beam expander and telescope design.

We believe our laser design provides a serious alternative to the alexandrite and dye laser systems which have been used for atmospheric iron measurements in the past. While alexandrite lasers are built only by few specialized companies, diode-pumped Nd:YAG technology has been developed and improved for many years and is now readily available. Dye lasers have the obvious disadvantage of high maintenance work and are thus considered unsuitable for the new generation of automatic and low-maintenance lidar instruments. Concerning spectral properties, our Nd:YAG laser is similar to existing alexandrite lasers. Both laser types emit pulses of several hundred nanoseconds length and are therefore spectrally very narrow (few MHz). This characteristic makes these lasers ideally suited for spectroscopy of atomic absorption lines and thus atmospheric temperature and wind measurements. Taking into account the fact that our laser prototype uses only one pump chamber, the output power (5 mJ at 100 Hz) is in the same order of magnitude as alexandrite lasers described in [14] (85 mJ at 25 Hz, two pump chambers) and [13] (100 mJ at 34 Hz, two pump chambers, not longitudinal single-mode). With spectral properties and power output being roughly equal, we think the main benefit of using diode-pumped Nd:YAG lasers in new iron lidar systems is the higher power efficiency which facilitates a more compact laser design. So far all iron lidar systems were based on flashlamp-pumped lasers which require more powerful power supplies and cooling systems compared to typical diode-pumped lasers. The compactness and energy efficiency of our design is especially important for future airborne lidar systems such as the Airborne Lidar for Studying the Middle Atmosphere (ALIMA) which is currently under development at the German Aerospace Center (DLR).

Funding. The development of the laser system was funded by the German Aerospace Center (DLR).

Acknowledgements. The authors thank C.-Y. She and two reviewers for comments.

REFERENCES

1. M. R. Bowman, A. J. Gibson, and M. C. W. Sandford, Nature **221**, 456 (1969).
2. A. J. Gibson, L. Thomas, and S. K. Bhattachacharyya, Nature **281**, 131 (1979).
3. K. Fricke and U. von Zahn, Journal of Atmospheric and Terrestrial Physics **47**, 499 (1985).
4. R. E. Bills, C. S. Gardner, and S. J. Franke, Journal of Geophysical Research: Atmospheres **96**, 22701 (1991).
5. C. Y. She, J. R. Yu, H. Latifi, and R. E. Bills, Appl. Opt. **31**, 2095 (1992).
6. C. Y. She and J. R. Yu, Geophysical Research Letters **21**, 1771 (1994).
7. C. Y. She, J. D. Vance, B. P. Williams, D. A. Krueger, H. Moosmüller, D. Gibson-Wilde, and D. Fritts, Eos, Transactions American Geophysical Union **83**, 289 (2002).
8. Y. Xia, L. Du, X. Cheng, F. Li, J. Wang, Z. Wang, Y. Yang, X. Lin, Y. Xun, S. Gong, and G. Yang, Opt. Express **25**, 5264 (2017).
9. T. D. Kawahara, S. Nozawa, N. Saito, T. Kawabata, T. T. Tsuda, and S. Wada, Opt. Express **25**, A491 (2017).
10. D. A. Krueger, C.-Y. She, and T. Yuan, Appl. Opt. **54**, 9469 (2015).
11. C. Granier, J. P. Jegou, and G. Megie, Geophysical Research Letters **16**, 243 (1989).
12. M. Alpers, J. Höffner, and U. von Zahn, Geophysical Research Letters **17**, 2345 (1990).

13. X. Chu, W. Pan, G. C. Papen, C. S. Gardner, and J. A. Gelbwachs, Appl. Opt. **41**, 4400 (2002).
14. J. Lautenbach and J. Höffner, Appl. Opt. **43**, 4559 (2004).
15. B. Kaifler, F.-J. Lübken, J. Höffner, R. J. Morris, and T. P. Viehl, Journal of Geophysical Research: Atmospheres **120**, 4506 (2015). 2014JD022879.
16. S. Singh, R. G. Smith, and L. G. Van Uitert, Phys. Rev. B **10**, 2566 (1974).
17. Z. Wang, Y. Bo, S. Xie, C. Li, Y. Xu, F. Yang, J. Xu, Q. Peng, J. Zhang, D. Cui, and Z. Xu, Applied Physics B **104**, 45 (2011).
18. W. Liu, D. Zhang, J. Li, Y. Pan, Y. Bo, C. Li, B. Wang, Q. Peng, D. Cui, and Z. Xu, Optics & Laser Technology **46**, 139 (2013).
19. E. S. Fry, Q. Hu, and X. Li, Appl. Opt. **30**, 1015 (1991).
20. C. S. Gardner and F. A. Vargas, Appl. Opt. **53**, 4100 (2014).